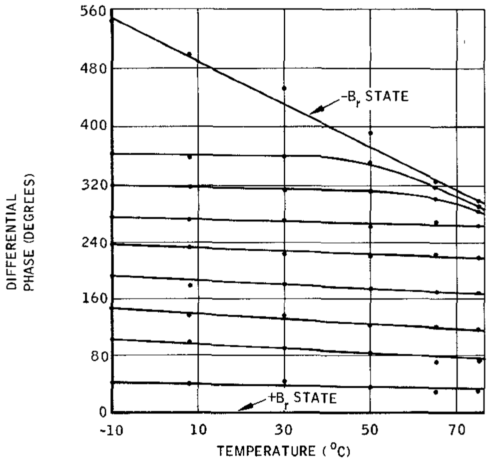

Fig. 12. Lithium-ferrite phase shifter. Differential phase versus temperature with flux drive.

the garnet. The only significant disadvantage to this lithium-ferrite material is that its temperature sensitivity (Fig. 11) is almost twice as high as garnets. With flux drive, however, very good temperature stability can be obtained over wide temperature ranges, as shown in Fig. 12.

CONCLUSIONS

For S-band phased-array applications of moderate element power ($\leq$5-kW peak), the foil-wrapped lithium-ferrite phase shifter with flux drive is an excellent choice with superior performance at low cost.

REFERENCES

[1] E. Stern, "Nonreciprocal remanence phase shifters in H-guide," in *1967 G-MTT Int. Microwave Symp., Dig. Tech. Papers* (Boston, Mass.), May 8–11, 1967, pp. 115–116.
[2] D. H Temme, R. L. Hunt, R. G. West, and A. C. Blankenship, "A low cost latching ferrite phaser fabrication technique," in *1969 G-MTT Int. Microwave Symp., Dig. Tech. Papers* (Dallas, Tex.), May 5–7, 1969, pp. 88–96.
[3] J. Frank, J. H. Kuck, and C. A. Shipley, "Latching ferrite phase shifter for phased arrays," *Microwave J.*, pp. 97–102, Mar. 1967.
[4] W. J. Ince, D. H. Temme, F. G. Willwerth, and R. L Hunt, "The use of manganese-doped iron garnets and high-dielectric constant loading for microwave latching ferrite phasers," in *1970 G-MTT Int Microwave Symp., Dig. Tech. Papers* (Newport Beach, Calif.), May 11–14, 1970, pp. 327–331.
[5] L. Stark *et al.*, "Microwave components for wide-band phased arrays," *Proc. IEEE* (*Special Issue on Electronic Scanning*), vol. 56, pp. 1908–1923, Nov. 1968.
[6] J. J. Green, "Microwave properties of partially magnetized ferrites," RADC-TR-68-312, Final Rep., Aug. 1968.
[7] D. H. Temme, G. F. Dionne, W. E. Courtney, G. Argentina, and P. D. Baba, "Lithium ferrites for microwave devices," in *1971 G-MTT Microwave Symp., Dig. Tech. Papers* (Washington, D. C.), May 16–19, 1971, pp. 74–75.

Practical Aspects of Phase-Shifter and Driver Design for a Tactical Multifunction Phased-Array Radar System

NORMAN R. LANDRY, MEMBER, IEEE, HUNTER C. GOODRICH, SENIOR MEMBER, IEEE, HENRY F. INACKER, MEMBER, IEEE, AND LOUIS J. LAVEDAN, JR.

***Abstract*—Three microwave garnet phase-shifter designs are used in the AEGIS weapons system. The microwave design is straightforward except that the toroid assembly is potted with silicone rubber to increase its power-handling capability and the magnetizing wires are shielded with a spiral-wrapped wire to prevent the propagation of higher order modes. The driver circuit uses a new "flux-feedback" concept for improved accuracy and employs monolithic circuits, hybrid circuits, and discrete components. Mechanical and electrical design of the interfaces with mating components are important cost considerations and the chosen designs are described in detail. Several techniques for improving production yield are discussed and a table of production statistics is provided. Performance histograns and data averages as a function of time and operating frequency are also presented.**

Manuscript received September 4, 1973; revised December 17, 1973. This work was supported by the U. S. Navy under Contract N00017-70-C-2403.
N. R. Landry, H. C. Goodrich, and H. F. Inacker are with the RCA Corporation, Moorestown, N. J. 08057.
L. J. Lavedan, Jr., was with the RCA Corporation, Moorestown, N. J. 08057. He is now with the Naval Research Laboratory, Washington, D. C. 20375.

INTRODUCTION

THE DESIGN and production of phase shifters and drivers for a large tactical phased array involves the resolution of a matrix of technical and economic problems. For the AN/SPY-1 array the requirements for a viable design include low unit cost and high production yield; high phase accuracy with respect to manufacturing spread, operating environment, and long-term drift effects; small size and weight; ruggedness and reliability for shipboard environment including conformance with military specifications; on-line monitoring; and compatible interface with a multifunction radar system. This combination of requirements has been met in the designs to be described. The

TABLE I
SPECIFICATIONS AND PRODUCTION STATISTICS FOR AN/SPY-1 PHASE SHIFTERS AND DRIVERS

	ANTENNA PHASER		RECEIVE PHASER		TRANSMIT PHASER	
	SPEC	STATISTICS	SPEC	STATISTICS	SPEC	STATISTICS
Freq (GHz) (Classified)	-		-		-	
VSWR, Max	1.35	1.25	1.25	1.11	1.25	1.10
IL, Ave (dB)	1.1	0.94	0.9	0.88	1.2	0.80
IL, Peak (dB)	1.5	1.11	1.2	1.06	1.5	1.00
# Bits	5	5	5	5	5	5
ΔØ Error (deg. rms)	9.5	5.1	4.5	2.00	4.5	3.2
IP Error (deg. rms)	14.2	8.7	4.0	2.7	4.0	2.3
Power, Ave (watts)	12	12	-	-	120	120
Power, Peak (KW)	1.5	1.5	-	-	15	15
Power, Peak Survive (Kw)	6.0	16.0	10.0	16.0	40	80
Temp, Operating (°F)	80 to 160	80 to 160	80 to 105	80 to 105	80 to 105	80 to 105
Temp, Survive (°F)	-80 to 167	-80 to 167	-80 to 167	-80 to 167	-80 to 167	-80 to 167
Sw. Speed, Reset (usec)	10 for both	4	7	5	13	6
Sw. Speed, Set (usec)		2	6	3	10	4
Sw. Rate, Ave (Hz)	800	800	800	800	800	800
Sw. Energy, Per PRF (u joule)	-	600	-	600	-	800
Sw. Current, Peak (amp)	13 +1	13	-	13	-	18
MTBF (hrs.)	88,700	-	83,333	-	83,300	-
Shock	MIL-STD-202D		MIL-STD-202D		MIL-STD-202D	
Vibration	MIL-STD-167		MIL-STD-167		MIL-STD-167	
Humidity, Dewpoint (°F)	50		50		50	

Note: Statistic values for phase include an estimate for measurement error, power-supply drift, and aging.

task has been found much more demanding and comprehensive than the development of a laboratory model phase shifter and driver.

Meeting the system specifications has required innovation and numerous design tradeoffs since no one parameter can be emphasized to the point where other requirements are compromised. Attempting to cut costs with a marginal design and risking poor production yields would be false economy. Likewise, failing to meet stability and reliability requirements would endanger the effective operation of the AEGIS weapons system.

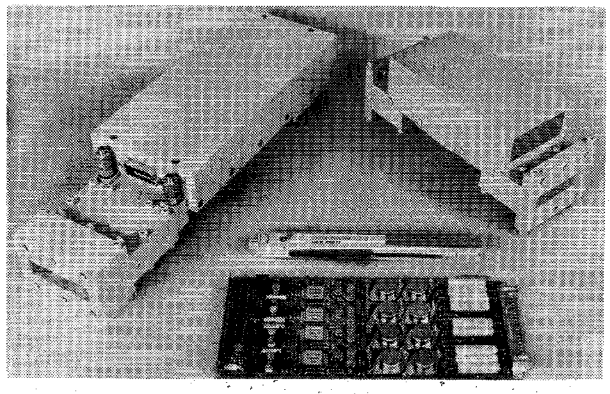

Fig. 1. Three phase-shifter designs. At upper left is a transmit phase-shifter assembly; at the right is a receive phase-shifter assembly; in the middle is an antenna phase shifter; and at the bottom, drivers for 4 antenna phase shifters.

MICROWAVE DESIGN

The AN/SPY-1 phased-array radar uses subarray steering to minimize the number of phase commands that must be generated. This requires three phase-shifter designs (Fig. 1). Transmit phasers are used at the inputs to the final cross-field amplifier tubes, receive phasers are used at the inputs to the receive beamformer, and antenna phasers are associated with each radiating element.

The three phase-shifter designs are of the waveguide, nonreciprocal flux-drive latching-garnet variety [1]. The garnet used is manufactured by Trans-Tech, Inc., and is their G-1004 with manganese substitution [2]. Each phaser has a rectangular toroid mounted in the center of a rectangular waveguide. The toroid slot contains two magnetizing wires and is otherwise filled with a ceramic that has a relative dielectric constant of 50, except for the transmit phaser for which the dielectric constant is 16. An impedance-matching transformer is used at each end of the toroid to provide a low VSWR over the frequency band of operation. The transmit and receive phase shifters require greater phase accuracy than the antenna phaser since each of their errors affects the performance of an entire subarray. To accomplish the greater accuracy, these units have sturdy housings with waveguide interfaces and have a mated driver which is adjusted during production for optimum performance. Specification values and production test statistics can be found in Table I which is discussed in a subsequent section.

Phase-shifter design usually starts with the selection of the toroid and waveguide cross sections. Using an analytical model [3], [4] to determine the phase-shifter cross section, a number of characteristics were studied:

1) differential phase versus frequency;
2) power-handling capability;
3) propagation of higher order modes;
4) matching transformer design;
5) toroid switching requirements.

Other considerations included in the overall set of tradeoffs were:

1) ferrite versus garnet;
2) temperature stabilization;
3) mechanical system constraints;
4) accuracy requirements;
5) production yield.

For these three designs, toroid and waveguide geometries were chosen to provide a nearly constant differential phase shift versus frequency characteristic. High dielectric-constant inserts [2], [5] were used to reduce phase-shifter size, weight, switching requirements, and cost. Garnet was chosen over magnesium–manganese ferrite because of the difficulty encountered in controlling the operating temperature in a tactical environment to within 20°F as required for the ferrite design. Matching transformers for the waveguide phase shifters were designed by setting the width of the garnet slabs to zero in the analytical model and calculating the propagation constant and impedance for dielectric loading only.

A calculation for the antenna phaser shows that an electric-field strength of 3020 V/in can be expected at the required peak power level of 6 kW. Across small air gaps, this field strength is multiplied by the dielectric constant of the inserts and becomes 151 kV/in. From Cobine [6], a 40-mil air gap should have a breakdown strength of 114 kV/in, while that of a 4-mil air gap is 240 kV/in. To insure that all air gaps are small, the toroid assembly is potted with a silicone rubber that is injected under pressure. This encapsulant tends to fill all air gaps and reduces the voltage stress by its dielectric constant, which is 2.6. The resulting stress in the silicone is about 60 V/mil, while its rating is 550 V/mil. All three designs are potted for improved power-handling capability and reliability.

The plot of insertion phase versus toroid magnetization shown in Fig. 2 illustrates a shortcoming of the analytical model. The discrepancy results from assuming that magnetization is uniform across the toroid leg, while actually the squareness of the B–H loop requires switching to start from the internal edge of the toroid and progress outward. The model provides one curve, whereas experimental data give two curves depending on whether the initial magnetization is clockwise or counter-clockwise. The two experimental curves are useful in describing the phase characteristics of a nonreciprocal phaser. The curve labeled "forward" has a nearly linear characteristic and is the one used in generating differential phase shift. In setting phase, the driver first wipes out the "past history" of the toroid by driving it to the maximum negative magnetization point. The driver then meters out a precise change in magnetization which results in the desired change in insertion phase. In order to use the curve labeled forward for both transmit and receive, the direction of current flow during corresponding drive pulses is reversed. This change in direction of the drive current compensates for the change in direction of the microwave energy between transmit and receive operations.

Referring to Fig. 2, as temperature is increased, the maximum remanent magnetization is decreased and the extremities of the curves are reduced. To a first-order approximation, the curve labeled forward decreases its slope slightly and the curve labeled "reverse" moves upward to close the two curves at their extremities. This tends to stabilize insertion phase over temperature and

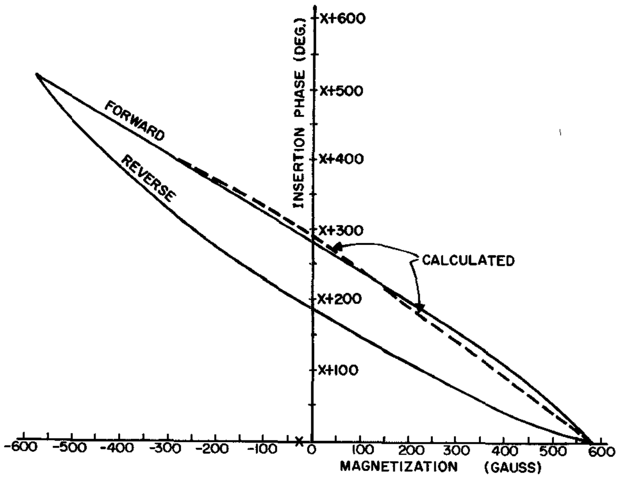

Fig. 2. Insertion phase versus magnetization, antenna phaser, calculated and experimental.

is the result of several compensating effects. The two-way electrical length, sometimes called reciprocal phase, at any bit setting is the sum of the insertion phases represented by the two curves. This characteristic may be important in some applications and for the antenna phaser amounts to a variation of ±30° over all bit settings.

Since toroid remanence determines the phase state of a phase shifter, all factors which affect remanence are of interest. One of these factors for a garnet toroid is magnetostriction. Whenever a garnet toroid of the G-1004 family is stressed, remanence changes. Remanence can be made to increase with proper stress but normal use tends to cause shear stresses which can greatly reduce remanence and phase shift. These three designs overcome the magnetostriction problem by using a compliant housing which allows relative motion between the garnet toroid and the housing as they expand and contract with temperature. In the case of the antenna phaser, external mechanical stresses are reduced by the use of a mounting spring at one end and a pair of support springs at the other end.

RF leakage from the antenna phaser had to be kept low since the array construction essentially places the 4480 phasers in a uniform distribution within a 12-ft-diam cavity that is about 6 in long. Most leakage comes from the magnetizing wires so these are covered (external to waveguide) with an iron-loaded silicone rubber. This covering also protects the phaser wires and lowers the Q of the array cavity. Total leakage from a phaser was measured as −35 dB at its worst frequency and as −40 dB when averaged over the frequency band.

Another problem associated with garnet phase-shifter design is the potential existence of narrow VSWR and insertion-loss spikes within the operating band of frequencies. These resonances are due to the propagation of undesired modes within the garnet-loaded portion of the phaser. These phase shifters were designed so that only one higher order waveguide mode (LSE_{11}) and the coaxial mode which can be supported by the magnetizing wires and the waveguide housing could propagate. The magnetizing wires are shielded along their entire length with a spiral-wrapped fine wire. This shield presents a larger resistance and inductance to longitudinal RF currents and effectively suppresses the undesired modes. To reduce coupling to these modes, a good fit between the inserts and the toroids and between the toroids and the housing must be obtained.

DRIVER DESIGN

Some of the primary requirements for the driver circuit include:

1) sufficient bidirectional control current to magnetize the phaser in the forward (see Fig. 2) direction for both the transmit and receive cycles;

2) control of the garnet-toroid magnetization with a long-term accuracy of 1–2 percent despite aging effects, temperature and supply voltage variations, and large garnet permeability changes;

3) completion of a RESET/SET cycle within 10 μs to meet the system minimum-range specification.

Fig. 3 illustrates the magnetic cycle through which the garnet toroid is driven during a transmit/receive sequence. The toroid is first set to the major-loop remanent or reference state B_{rt}. This is accomplished by energizing winding A with a RESET pulse whose magnetizing force is several times the garnet coercive force. This is followed by energizing winding B with the transmit SET pulse, which has an amplitude e_0. During the pulse the toroid flux changes at a rate $d\phi/dt = e_0$. When the flux has changed the commanded amount ($\Delta\phi_t$ plus a small fall-back increment $\Delta\phi_f$) the driver pulse is terminated. The phaser is now ready for the transmit RF pulse. The magnetization direction of the RESET and SET pulses are reversed for receiving to compensate for the change in direction of the propagating RF energy.

The flux-feedback concept [7] was developed to achieve accurate flux control in a reliable and economical manner. The dual windings A and B are used for bidirectional magnetization of the garnet core. For RESET the appropriate amplifier A or B is gated on. The magnetizing current flows through a sampling resistor R_S. The voltage across R_S is applied to an integrated-circuit RESET comparator, which is also supplied with a reference voltage. When the desired RESET current level is reached, the voltage across R_S exceeds the reference, causing the comparator to change state and turn off the gated amplifier.

When the phaser is to be SET for a given phase shift, an analog command voltage, proportional to the desired phase shift, is applied to an integrated-circuit SET comparator. The appropriate amplifier is next gated on, and the undriven winding A or B is used as a sense winding to measure the level of flux change. This winding develops a voltage, $e_S = -d\phi/dt$, that is exactly equal to the instantaneous rate of flux change. This voltage is integrated via R_1C_1 to produce a voltage ramp. The level of the integrated voltage at any instant is proportional to

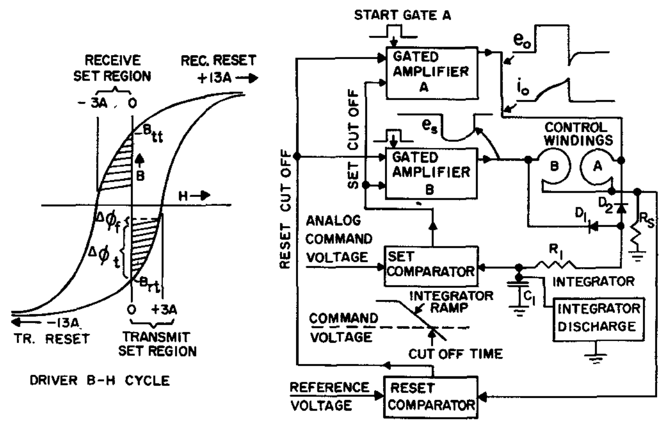

Fig. 3. Flux-feedback driver.

the amount of flux that has been switched. When the switched flux builds to the commanded level, the integrated voltage exceeds the analog command voltage, causing the SET comparator to change state and quickly turn off the gated amplifier.

In the flux-feedback approach, driver accuracy is primarily determined by the SET comparator threshold and the integrator time constant R_1C_1. Long-term stability can be readily achieved for these parameters. Substantially eliminated as causes of flux variation are normal garnet permeability changes, amplifier temperature and aging effects, drive lead voltage drop, and supply voltage fluctuations as thousands of high-current drivers switch simultaneously. Limitations on the accuracy of the flux-feedback approach are posed by variations in amplifier cutoff time, waveform distortion in the sense-winding leads, variations in fallback flux, uncompensated nonlinearity in the phase shift versus flux characteristic, and integration imperfections introduced by the finite R_1C_1 time constant. In practice, these errors have proven quite small. Flux-feedback drivers built with discrete components, thick-film hybrid integration, and monolithic integration have all given consistantly accurate performance (see Table I).

MECHANICAL INTERFACES

Mechanical packaging of the phase shifters into the array antenna often requires special input and output matching structures. The transmit and receive phase shifters mate with waveguide components and pose no special problems. The antenna phaser, however, must provide an end-launched coaxial connector [8] at one end to mate the loaded waveguide to a coaxial power divider and a blind connection with a radiating horn at the other end where no mechanical fasteners are allowed.

The coaxial connector, exciter, and transformer, together with a phase shifter inserted in a breadboard radiating horn, are shown in Fig. 4. The coaxial connector, exciter, and transformer were designed empirically. The resultant connector has a 60-Ω section, the exciter has a trapezoidal cross section, and the transformer has a di-

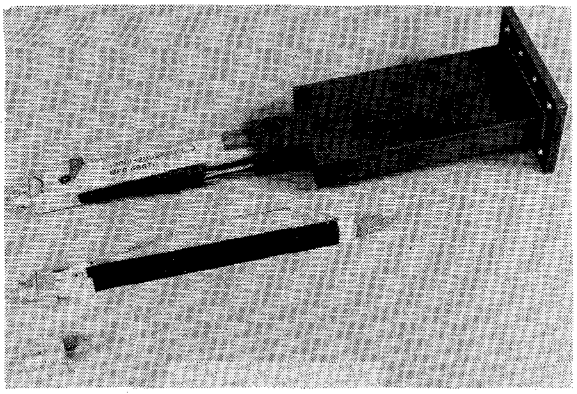

Fig. 4. Antenna-phaser interfaces.

electric constant of 16. The transformer is bonded to the garnet stack. The connector butts against the transformer, with the exciter fitting into the transformer slot and attaching to one of the waveguide broadwalls with a small screw. The exciter shape provides the capacitance required between the exciter and the side walls of the transformer for impedance matching and automatically provides centering of the exciter in the transformer slot. The exciter is formed through powder metallurgy, has no sharp edges, and preserves the high power handling capability of the garnet toroid assembly. Nickel plating is used on the coaxial center conductor to make it compatible with the gold plating in the power divider; the exciter is tin plated to make it compatible with the aluminum phaser housing. Nickel and tin also form a compatible couple.

The horn end of the phaser uses a standard two-step waveguide transformer. The first step is of ceramic and the second step is of Duroid. This end of the phaser slips into the radiating horn and uses nickel-plated stainless-steel spring contacts to make the connection between the phaser and horn. Electrical performance of this design provides a VSWR and insertion loss which are essentially independent of the position of the phaser in the horn. Insertion phase changes by $\pm 4.5°$ for a change in insertion depth of ± 0.062 in.

An assembly of a 32:1 power divider, 32 phase shifters, an electronics nest containing eight driver boards, a line-receiver board, and a voltage-regulator board with interconnecting wiring and support brackets is called an array module. The array is composed of 140 identical array modules. Fig. 5 shows a picture of an array module (supported by its assembly fixture) and a horn module. The horn modules are sealed at their radiating apertures and mount to the front of an array structure plate. The array modules are plugged in from the rear of the plate resulting in the requirement that 32 blind microwave connections be made simultaneously. To allow for misalignment and manufacturing tolerances, each phase shifter is mounted to the power divider with a spring clamp that allows up to $\pm 0.5°$ misalignment from perpendicularity. These spring clamps, together with the springs

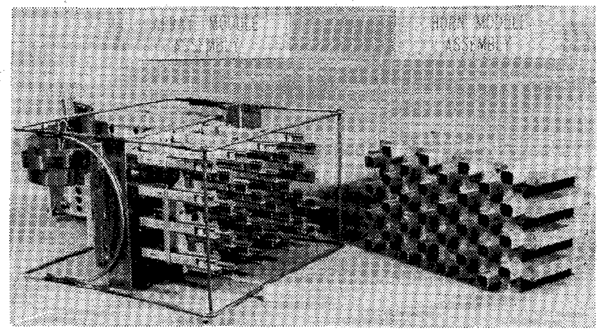

Fig. 5. Array-module and horn-module assemblies.

at the horn end of the phasers, satisfy the design constraints of providing self-alignment and self-connection between the two modules. Each of the horns in the horn module has a tapered input section to help in the alignment and support brackets are used to hold the phase shifters in nominal position when they are not engaged with the radiating horns. Fig. 5 also shows the flat ribbon cable that is used to connect the array module to the power and signal distribution systems. A similar low-impedance stripline is used to interconnect each phase shifter and driver. This design provides easy replacement of faulty phase shifters from the front of the array module.

ELECTRICAL INTERFACES

The successful design of a phase-shifter driver requires careful consideration of the interfaces with the rest of the radar system since, in fact, the overall design objective is a working system, not a set of isolated components. The three main driver interfaces are the output interface with the phaser load, the command input interface with the beam-steering controller, and finally, the power-supply interface.

The modular packaging concept for the array requires that the drivers be mounted in a nest assembly behind the 32:1 power divider. The drive leads are required to run from the driver through the power divider to the phaser resulting in drive lead lengths of about 18 in. Several schemes were considered: twisted pairs, coaxial cables, and printed striplines. The criteria were 1) to provide a low inductance interconnection between the driver output and the phaser, and 2) to provide a system compatible with normal factory assembly techniques. The design chosen consists of a flexible low-impedance two-layer printed stripline configured with the two drive leads on the top layer and the return lead on the bottom layer. The driver end of the stripline is compatible with solder termination and the phaser end contains pins for wire wrap to a mating assembly on the phaser.

Subarray steering requires that the beam-steering controller distribute precise analog signals to 128 corresponding elements in each of 32 subarrays. In order to minimize the number of analog drivers and interface cables, 128 analog commands are "daisy chained" on the array with approximately equal loading on each line. Contamination of the analog signals is minimized by 1) sending the largest practical amplitude signal (about 15-V full scale) on the line and attenuating by 10:1 at the driver input; 2) controlling the transition times of the analog commands to prevent crosstalk between lines; and 3) using a controlled impedance flat ribbon cable with shields top and bottom to minimize external noise pickup.

In addition to the analog phase commands, several timing signals are required by the driver. These signals are also distributed with flat ribbon cable. Standard integrated-circuit balanced-current-mode line drivers and line receivers are used. Each array module contains a line-receiver card to convert the balanced line signals to single-ended T^2L levels and to provide the required fan-out for the 32 phase-shifter drivers.

Although the flux-feedback driver described in this paper is quite tolerant to power-supply variations, careful design of the power-distribution network is required to insure an operating system. Since each driver is required to switch about 13 A for each RESET command, over 50 000 A are required for the entire array in the span of a few microseconds. The pulse nature of the current transient requires the use of local energy-storage elements at each driver to reduce the transient-current demands on the system power supply.

The array power-supply system consists of an unregulated main supply with energy storage consisting of local decoupling capacitors at each driver and also a high-efficiency switching mode regulator located in each array module. The decoupling at the driver reduces the 13-A peak to 0.5-A peak with an average value of 48 mA for a switching rate of 1 kHz. The local regulator reduces the 16-A peak current for 32 drivers to a peak of 0.5 A with an average value of 1.5 A/kHz.

An important consideration in the design of the dc power system for a tactical array is that of preventing localized component failures from propagating through the system, possibly resulting in power shutdown. To prevent this occurrence, each power input point on all modules used in the array is buffered with a small, fusable resistor which opens in case of circuit malfunction (e.g., shorted transistors, capacitors, etc.) and effectively disconnects the malfunctioned circuit from the power supply.

DRIVER MONITORING

The unique characteristic of a phased array, that is, the combining of energy from many thousand radiating sources to form a useful radar beam, poses a difficult problem in the detection of individual malfunctioned elements. A substantial number of elements can be inoperative with relatively small degradation of the overall beam pattern. Proper maintenance philosophy requires that malfunctioned elements be detected before the system performance becomes degraded. Again the phased array presents a unique problem, since, due to the large number of elements involved, manual fault detection is impractical and some form of automatic monitoring must be provided to detect and localize faulty elements.

The monitoring system implemented in the AN/SPY-1 array uses digital integrated circuits, located on each driver module to check the operation of the SET and RESET comparators, described earlier, for proper operation every time the driver is switched. If any malfunction occurs in any of the four drivers on a common board, a digital signal is developed to inform the monitoring system of the malfunction. These signals are linearly summed at each array module to develop a voltage proportional to the number of defective driver boards in each array module. The outputs of each of the 140 array modules are periodically scanned by the monitoring system to generate a running tally of the number of failures and their location.

The monitoring system accumulates the number of failures in each array module; however, it cannot tell which of the driver boards within an array module is defective. To facilitate maintenance, a lamp is included on each driver board. The maintenance technician obtains a printout of the locations of array modules containing defective drivers from the monitoring system, goes to the array, and replaces driver boards showing lighted monitor lamps. In this way, no manual troubleshooting is required and maintenance time and manpower requirements are minimized.

The built-in monitoring at each driver is also capable of detecting certain phase-shifter faults as well as system malfunctions such as faulty or missing commands, missing gate signals, defective power-supply voltages, and is capable of checking itself through proper programming. The benefits of a fully automatic system far outweigh the added cost of about 3 percent of driver cost.

PRODUCTION CONSIDERATIONS

The overriding design consideration for production is cost. The major factors affecting cost are yield, assembly and test time, and defects requiring repair. Several techniques for maintaining and improving production yield are being used. In addition to the normal purchased material inspection, these include care in assembly, in-line assembly inspection and test, and quality-control procedures.

Each phase-shifter assembly is made up of multiple sections of garnet toroids to obtain the required total length. The antenna and receiver phasers utilize the same garnet assembly consisting of three toroid sections, while the transmit phaser is made up of five sections.

One in-line test is the measurement of maximum remanent magnetization of all garnet toroid sections delivered by the manufacturer and appropriate categorization. By proper selection it is possible to mate toroids with below-average remanences with specimens of above-average performance. Thus toroid sections purchased with a remanence tolerance of ±5 percent (a tolerance acceptable to high yield by the toroid manufacturer) are assembled to yield a device with a remanence tolerance of less than ±2.5 percent. The resultant end product using toroids thus selected will exhibit minimum deviation from the nominal flux-phase response.

Secondly, to further improve yield the completed antenna phase shifter is also categorized into three groups as to flux-phase response when driven by an "average" driver. These categories may be labeled A, B, and C, for example. Type A would provide too much differential phase for a level of switched flux, type B is average, and type C would provide too little. It is possible to mate A and C categories with appropriately adjusted drivers to produce an average response. Because of the packaging design (four drivers per circuit board and a nest of drivers for each array module), this pairing of driver and phase shifter is accomplished in groups of 32 units and each array module is appropriately marked.

A third technique is the trim of inherent insertion phase of the microwave hardware. Since driver and phase shifter are not a mated pair for the antenna phaser design, this trim must be accomplished as part of the phase shifter independent of driver. This is done with inductive iris triplets that can be inserted into the side of the phaser housing. Positions for three sets of triplets are available thus permitting a trim range of ±24° in steps of 8°. Insertion-loss variation due to use of these irises is approximately ±0.04 dB and VSWR effects are negligible. The receiver and transmitter phase-shifter designs have mated phasers and drivers permitting insertion and differential phase trim to be simply accomplished by electronic methods. This allows precise adjustment at time of test for minimum phase error.

After completion of in-line electrical inspection (check for charging wire continuity and selection of irises for insertion phase trim) and a thorough mechanical inspection, each phase shifter is subjected to electrical test on a Hewlett-Packard Automatic Network Analyzer [9]. Special features have been added to the standard test hardware and programs to permit automatic control of the driver from the analyzer computer and to record all data on magnetic tape for future statistical processing.

To accomplish the specific test of phase shifters, computer measurement programs with the following features have been written.

1) Calibration of the measurement system where each port of the device to be tested is different (the antenna phaser has a coaxial input connector and mates with a waveguide horn at its output).

2) Measurement flexibility by manual switch option (five frequencies and eight phase states or nine frequencies and 32 phase states).

3) System check of driver power-supply voltages.

4) Real-time test and graphic display (under computer control) of combined performance for driver alignment.

5) Lockout of data taken on reference units for system checks.

6) Correction of data for variations in test environmental temperature and scaling performance to actual radar environment.

7) Automatic categorization of phase shifters based on flux-phase response.

8) Automatic accept/reject decision based on programmed-in specification limits to eliminate operator judgement.

9) Computation of average performance data.

10) Computation of running rms differential phase and standard deviation of insertion phase over all units previously evaluated.

11) Recording of all pertinent data on magnetic tape.

In addition to these acceptance test programs, other programs have been written for design evaluation and qualification testing of all phasers and drivers. These programs are specifically oriented to on-line adjustment and evaluation of the unit under test for various test conditions.

PERFORMANCE DATA

Data measured on production units of the three phaser and driver designs show that differential phase shift is linear with command and frequency within an rms error of less than 2.5°. Adding the differential phase error due to random mating of antenna phasers and drivers, this value is still less than 3.5° rms. Table I lists the specification requirements and typical performance of the three designs. Differential and insertion phase errors include the effects of ambient temperature, RF power, dc power-supply drift, and an estimate for aging. Phase errors for the antenna phaser are far below specification values. This is attributable to the limited production (5000 units) where each constituent part is purchased from one vendor. As the number of suppliers is increased, a greater variability in performance data is expected. Switching energy includes that which is delivered to the toroid and switching wires as well as driver efficiency. The mean time between failures (MTBF) for the antenna phaser and driver is allocated as 200 000 h for the phaser and 160 000 h for the driver. Since they are not a mated pair, faulty drivers can be replaced during normal maintenance while defective phasers will await depot replacement. Testing during vibration indicated several small mechanical resonances, but these had no measurable effect on performance characteristics. All power-handling requirements were exceeded during test to assure adequate margin for unit-to-unit variations.

Typical arc-over of the antenna phaser is in excess of

10 kW into a short circuit and that for the transmitter phaser is estimated to be 80 kW under normal operating conditions. The transmit phaser was subjected to 2-h cobalt radiation at full rated power with no change in performance.

Temperature performance profiles were measured as part of qualification and are as follows:

	Antenna	Receiver	Transmitter
$\Delta\theta$—latch to latch	−0.158 percent/°F		
$\Delta\theta$—(any bit flux)	−0.0933 percent/°F	−0.075 percent/°F	−0.073 percent/°F
Insertion phase	−0.178 deg/°F	0.0	−0.22 deg/°F
Insertion loss	−0.0034 dB/°F	−0.0051 dB/°F	−0.0042 dB/°F

Fig. 6 is a multiple histogram depicting performance measured on the production antenna phasers. The largest nonsymmetry can be seen in the single-unit rms differential phase error. A small number of units produced were beyond the limit of 6.0° for category *B*, but these were accepted after the computer recategorized them as category *A* or *C*. Final production yield of the antenna phasers and drivers was about 98 percent.

Fig. 7 is a plot of cumulative rms differential phase error and standard deviation of insertion phase as a function of number of units produced (time). Also included is a plot of the rms error of a reference phase shifter repeatedly measured throughout production to monitor test-facility repeatability and performance. The rise in the reference curve near the end of production was traced to a degraded microwave switch in the measurement system which was insufficient to create faulty calibrations but which produced random erroneous readings. This rise in test-system error should also account for the rise in cumulative rms error near the end of production. The dip in the rms error curve near the beginning of production is due to the small number of units evaluated and also due to the fact that the "average" driver flux was established based upon these first units. The shape of the insertion phase curve is reasonable when it is realized that in order to assure continued acceptable error, each unit was tested to absolute limits and those possessing larger errors were removed from further test and placed on hold. When the standard-deviation trend was established as acceptable, the individual unit criteria were modified to then accept units of greater individual error, resulting in an increasing error curve.

Fig. 8 is a plot of the parameters of VSWR, insertion loss, and standard deviation of the insertion phase as a function of frequency. Where applicable, the values recorded are also averaged over all phase states at each frequency. The shape of the insertion-phase response was expected since original iris selection for minimum error was performed at midband.

All phaser and driver designs have been successfully subjected to thorough qualification testing including microwave-power evaluation and environmental performance under humidity, temperature, shock, and vibration.

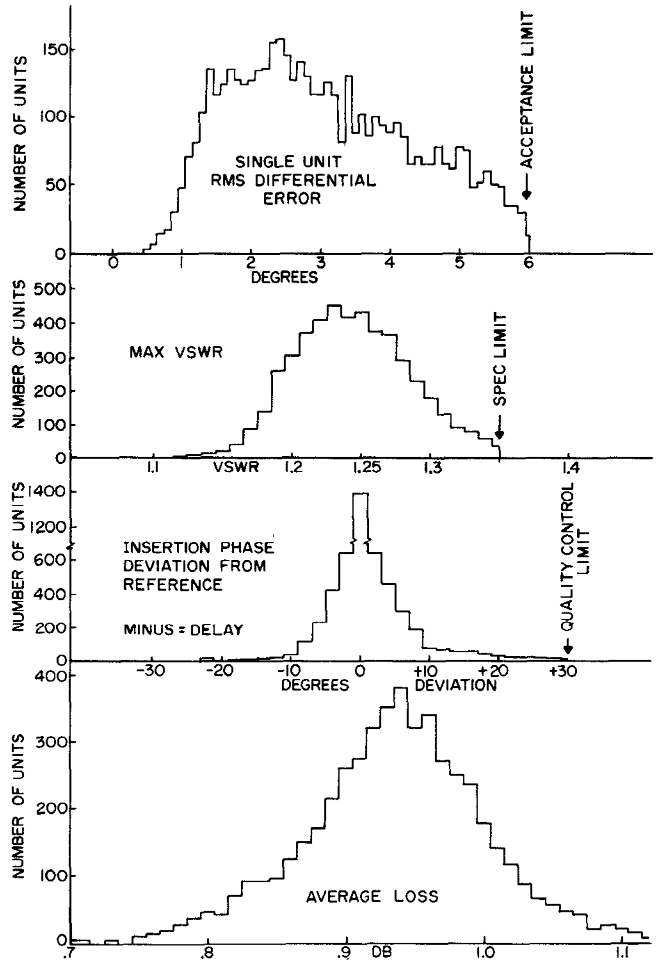

Fig. 6. Antenna-phaser production performance histograms.

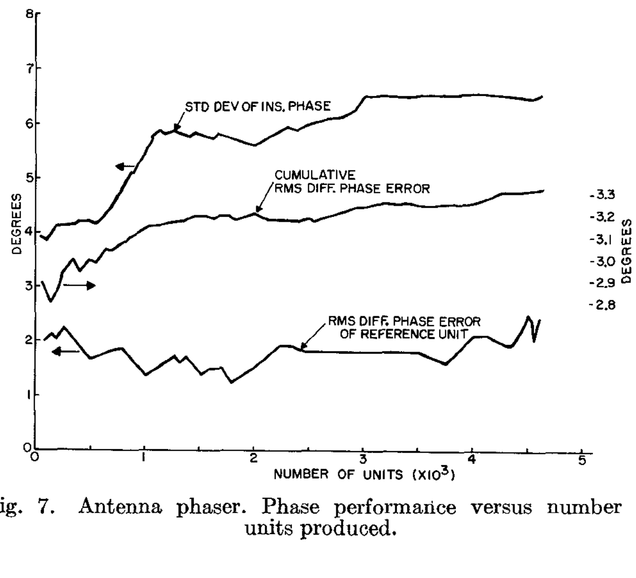

Fig. 7. Antenna phaser. Phase performance versus number of units produced.

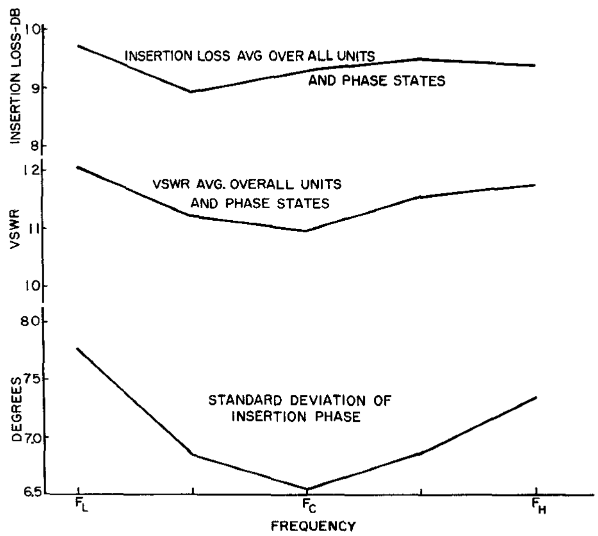

Fig. 8. Frequency performance of antenna phaser.

CONCLUSIONS

Both the electrical- and mechanical-design concepts employed in the design of the drivers and phasers described in this paper have been validated in the production of an operating state-of-the-art phased-array antenna. The close coordination maintained between engineering and manufacturing during the design and production phases allowed assembly of a most complex structure with a minimum number of problems.

The assigned component tolerances, error budgets, and automated testing techniques employed during driver and phaser production have also been validated by extensive pattern testing of the completed array assembly. Finally, the array has been integrated into the radar system and has demonstrated multifunction capability as a system component.

Manufacturing costs for the phase shifter have been studied for each step of the fabrication and test process. This analysis has resulted in a list of 15 areas of potential redesign to reduce production costs. About half of these ideas (with about one-third the savings) are relatively minor and entail very little risk. The other half involves substantial redesign which would be justified with an additional production of about 10 000 phasers. The garnet toroids account for more than 40 percent of the phaser material cost, hence several areas of interest are reducing toroid volume, developing alternate suppliers, and searching for a suitable ferrite. Yield from 100-percent phaser testing has been very high and reduced testing, sample testing, and testing at the array-module level are being considered.

The design of efficient cost-effective drivers requires a continuing design effort as advances in the semiconductor art make new and better components available. As part of this effort, a second monolithic design has been developed which can replace the thick-film hybrid-control circuit used in initial production. The monolithic development has obvious advantages both in producibility and reliability.

Further, the test data obtained during the initial production run have been analyzed, and, in some areas, the circuit far exceeds the design requirements. These data will be used to relax component tolerances and thereby reduce the production costs of future drivers.

ACKNOWLEDGMENT

The authors wish to thank their co-workers and supervisors for their assistance in this project. Particular thanks are due R. W. Martin, J. A. Bauer, E. Dixon, E. H. Poppel, D. R. Kline, J. C. Moore, and R. J. Tomsic.

REFERENCES

[1] W. J. Ince and D. H. Temme, "Phasers and time delay elements," M.I.T. Lincoln Lab., Lexington, Mass., Contract AF19(628)-5167, Project Rep. RDT-14, July 11, 1967.
[2] W. J. Ince, D. H. Temme, F. G. Willwerth, and R. L. Huntt, "The use of manganese-doped iron garnets and high dielectric constant loading for microwave latching ferrite phasers," in *G-MTT 1970 Int. Microwave Symp. Dig.* (Newport Beach, Calif.), May 11–14, 1970, pp. 327–331.
[3] W. J. Ince and E. Stern, "Nonreciprocal remanence phase shifters in rectangular waveguide," *IEEE Trans. Microwave Theory Tech.*, vol. MTT-15, pp. 87–95, Feb. 1967.
[4] L. R. Whicker and R. R. Jones, "Design guide to latching phase shifters," *Microwaves*, pp. 31–39, Nov. 1966; 43–47, Dec. 1966.
[5] N. R. Landry, "Microwave phase shifters," *RCA Eng.*, pp. 20–25, Oct./Nov. 1969, Reprint RE-15-3-5.
[6] J. D. Cobine, *Gaseous Conductors, Theory and Engineering Applications*. New York: Dover, 1958, p. 166.
[7] H. C. Goodrich and R. J. Tomsic, "Flux feedback boosts accuracy of phased array radar systems," *Electronics*, vol. 43, pp. 77–80, Nov. 23, 1970.
[8] G. J. Wheeler, "Broadband waveguide-to-coax transitions," in *IRE Nat. Conv. Rec.* (New York), Mar. 18–27, 1957, pt. 1, pp. 182–185.
[9] R. A. Hackborn, "An automatic network analyzer system," *Microwave J.*, pp. 45–52, May 1968.